GAP SOLITONS IN ASYMMETRIC DUAL-CORE NONLINEAR OPTICAL FIBERS

D.J. Kaup[1]
Institute for Nonlinear Studies, Department of Mathematics and Computer Science, and Department of Physics, Clarkson University, Potsdam, NY 13699-5815, USA

B.A. Malomed[2]
Department of Interdisciplinary Studies, Faculty of Engineering, Tel Aviv University, Tel Aviv 69978, Israel

ABSTRACT

A new nonlinear optical medium which can support gap solitons is proposed, an asymmetric dual-core fiber with opposite signs of the dispersion in its two cores, which can be easily fabricated choosing the carrier wavelength close to the zero-dispersion point. We consider soliton solutions, combining the analysis of the dispersion relation for the linearized system, the variational approximation for the full nonlinear one, and direct numerical methods. We find that in the case when the cores are asymmetric but still have the same sign of the dispersion, the general picture of the solutions is qualitatively the same as studied recently in the model with identical dispersions in the two cores, the asymmetry being solely accounted for by a phase-velocity mismatch between the cores. The case when the dispersion is zero in one core is special: in this case, the system's spectrum simultaneously has one semi-infinite and one finite gaps. In the most interesting case when the dispersion in one core is normal (and the system has only a finite gap in its spectrum), we find novel features of the gap soliton: its tails may be decaying with oscillations (which opens way to nontrivial bound states of the solitons), the energy in the soliton's normal-core component may be, quite counterintuitively, equal to or larger than the energy in the anomalous core, and a part of the gap where the solitons might exist remains empty, containing no actual soliton solutions.

[1]E-mail kaup@sun.mcs.clarkson.edu
[2]E-mail malomed@eng.tau.ac.il

1 INTRODUCTION

Gap solitons, i.e., solitons residing in a gap of the system's linear spectrum, have recently attracted a lot of attention in nonlinear optics [1]-[7]. The best-known example are the Thirring-type solitons in nonlinear optical fibers with a resonant Bragg grating, theoretically predicted in [2]. The first experimental manifestations of the nonlinear pulse propagation in the latter system were observed in [3], and soon after this, the full-fledged Bragg-grating solitons have been observed in [4]. [See also the state-of-the-art review [5].] Very recently, considerable effort has gone into the theoretical study of gap solitons in media with quadratic nonlinearity [6, 7], albeit one has yet to create solitons of this kind in a real experiment.

Another medium capable to sustain optical gap solitons is a nonlinear *asymmetric* dual-core fiber (DCF), provided that the two cores have opposite signs of the temporal dispersion, one core being normal and the other one being anomalous. Obviously, a normal-dispersion core cannot by itself support a bright soliton. However, this may be possible if it is linearly coupled to an anomalous-dispersion core. This possibility was briefly mentioned in Ref. [8]. Solitons in asymmetric DCFs were studied in detail in another recent work [9], but the model considered there only allowed an asymmetry in the form of a phase-velocity mismatch between the cores, while their dispersion were identical (anomalous). This type of the asymmetry in the dual-core fiber can be induced by elliptic deformations of the cores in mutually orthogonal directions, keeping the cores' cross-section areas equal [8]. The difference in the effective dispersion coefficients between the cores can be additionally generated by a small difference in their cross-section areas, with regard to the usual condition that each core operates close to its zero-dispersion point [10], hence the core's residual dispersion is highly sensitive to its cross-section area. One can thus generate dispersions the opposite signs in the two cores. Technologically, it is quite possible to fabricate such an asymmetric dual-core fiber under controllable conditions.

The objective of the present work is a theoretical study of the gap solitons in the asymmetric DCF, extended to the case where the dispersions in the cores can have opposite signs. The model, based on a system of two linearly coupled nonlinear Schrödinger (NLS) equations, is formulated in section 2. In the same section, we derive a dispersion relation for the linearized system. The gap solitons are expected to exist inside the system's spectral gaps. Solitons of two different types are predicted on the basis of the linear analysis: the usual ones with monotonically decaying tails, and solitons with decaying, but oscillating tails. The latter type of soliton proves to be possible only when the two dispersions have *opposite* signs. Similar solitons are known when the two cores of a DCF have equal dispersions, but with a *group*-velocity mismatch present [11]. The decaying oscillating tails can give rise to nontrivial bound states of the solitons (bi-solitons and multisolitons) [11]. In section 3, we formulate a variational approximation (VA) for the full nonlinear system. The VA has produced some very accurate results in previous studies of the solitons in both symmetric and asymmetric DCFs [8, 9]. We shall also use direct numerical solutions to verify the validity of the VA results. In section 3, we present the results obtained by means of the VA based on a Gaussian

ansatz, with different widths allowed for the two components of the soliton, along with some conclusions concerning the soliton's stability. A noticeable and somewhat counterintuitive result produced by the VA (and independently supported by other analytical arguments) is that, when the dispersion in one core is normal, the energy of the soliton's component in this core may be *equal to* or *larger than* the energy of the anomalous-dispersion component. Thus, the linear coupling to the anomalous core allows the normal-dispersion one to effectively support a bright soliton, which is evidently impossible in the absence of the coupling. Though this result seems counterintuitive, it can be understood because the linear coupling mixes the anomalous and normal components, which strongly changes the system's spectrum in the region where the gap exists. In fact, in this region one cannot unambiguously identify the two cores as anomalous and normal. Another noticeable and unexpected feature is that a part of the gap may remain unfilled with the soliton solutions (note, however, that a similar feature was recently found in the analysis of the gap solitons induced by the Bragg grating in the waveguides with the quadratic nonlinearity [6]).

In section 4, different types of the solitons predicted by the VA are verified by means of direct numerical methods. In accord with the predictions of the linear analysis and the VA, solitons with both monotonously decaying and oscillating decaying tails are found to exist. It is also found that "delocalized solitons", which are localized pulses superimposed on top of a continuous wave (CW) of a small but finite amplitude, also exist, as predicted by the linear analysis and the VA. These delocalized solitons have been recently found in the asymmetric model, where the asymmetry was produced solely by the phase-velocity mismatch [9].

2 THE MODEL AND ITS LINEAR ANALYSIS

We start with a general model of the asymmetric dual-core fiber, which can be written in the following form (cf. [8]):

$$iu_z + qu + icu_\tau + \frac{1}{2}u_{\tau\tau} + |u|^2 u + v = 0, \tag{1}$$

$$iv_z - \delta\left(qv + icv_\tau + \frac{1}{2}v_{\tau\tau}\right) + |v|^2 v + u = 0, \tag{2}$$

where $u(z,\tau)$ and $v(z,\tau)$ are envelopes of the electromagnetic waves in the two cores, z and τ are, as usual, the propagation distance and the reduced time, the linear-coupling constant has been set equal to 1, the dispersion coefficient in the first (anomalous) core is also normalized to 1, $-\delta$ is the relative dispersion coefficient in the second core (defined so that $\delta > 0$ corresponds to the normal dispersion in it), the parameters q and c measure, respectively, the phase and group velocity differences between the two cores (the corresponding terms in (2) are defined so that they include the multiplier $-\delta$ just for convenience, which is always possible except for the case $\delta = -1$, when the dispersions in the two cores are identical). The group-velocity difference can then be eliminated by means of the obvious

transformation $(u,v) \to (u,v)\ \exp(-ic\tau)$, while the phase-velocity mismatch q must be kept as an independent parameter.

There are various different physical sources for the asymmetries proposed in Eqs. (1) and (2) [8]. As it was mentioned above, the phase- and group-velocity differences can be generated by elliptic deformations of the two cores in orthogonal directions, upon keeping equal effective cross section areas and the same polarization of light in both cores. The deformation of the cores, affecting their modal structure, may also give rise to some difference in their dispersion coefficients. This difference can be essentially augmented by a relatively small mismatch in the cross section areas, which produces a negligibly weak effect on the nonlinear coefficients, but, assuming the fiber to operate near the zero-dispersion point, at which the terms produced by the material and waveguide dispersions nearly compensate each other [12], even a weak change of the latter term may significantly alter the effective dispersion coefficient.

The linear dispersion relations of Eqs. (1) and (2) determine a parameter range inside of which soliton solutions can exist. Substituting $u, v \sim \exp(ikz - i\omega\tau)$ into the linearized equations (10 and (2) yields

$$k = \frac{1}{4}(\delta - 1)\left(\omega^2 - 2q\right) \pm \sqrt{\frac{1}{16}(\delta+1)^2\left(\omega^2 - 2q\right)^2 + 1}. \tag{3}$$

Eq. (3) can be easily inverted, which is also a useful representation of the dispersion relation:

$$\omega^2 = 2q + \delta^{-1}\left[(1-\delta)\,k \pm \sqrt{(1+\delta)^2 k^2 - 4\delta}\right], \tag{4}$$

the signs $\pm$ in Eqs. (4) and (3) being the same. In the particular case $\delta = 0$, Eq. (4) is replaced by

$$\omega^2 = 2k^{-1}\left(qk + 1 - k^2\right).$$

A fully localized soliton solution is possible only for values of the propagation constant k that belong to the *gap* in the spectrum (3), i.e., such that neither value of ω^2 given by Eq. (4) will be real and positive. Moreover, if the values of ω^2 given by (4) are real and negative, then the soliton will have monotonically decaying tails. If, instead, the values of ω^2 are complex, then the tails of the resulting solitons will decay, but with oscillations. It then immediately follows from the above and (4) that when $\delta \leq 0$ (i.e., the dispersion of both cores is either anomalous or vanishes in one), *only* monotonously decaying tails are possible.

The oscillating tails are possible provided that $\delta > 0$, when the dispersion in the second core is *normal*. In particular, it follows from Eq. (4) that, in the *sub*gap

$$0 \leq k^2 < 4\delta/(1+\delta)^2 \tag{5}$$

existing at $\delta > 0$, *only* solitons with the oscillating decaying tails are possible. The existence of this type of the soliton for $\delta > 0$ will be confirmed by direct numerical results displayed below in section 4. The DCF soliton with the decaying oscillating tails is a new result

(previously, they were predicted in a model where the dispersion was the same in both cores, $\delta = -1$, but with a group-velocity mismatch between them [11], which is a special case not contained in Eqs. (1) and (2)).

The shape of the dispersion relation given by Eqs. (3) and (4) for $\delta < 0$ is quite obvious: it gives rise to a semi-infinite gap, extending to $k \to -\infty$. In the case $\delta = 0$ (no dispersion in the second core), the spectrum includes the semi-infinite gap at $k > \sqrt{1 + \frac{1}{4}q^2} + \frac{1}{2}q$, plus an additional finite gap at $-\left(\sqrt{1 + \frac{1}{4}q^2} - \frac{1}{2}q\right) < k < 0$ (Fig. 1). At $\delta > 0$ (the opposite dispersions in the two cores), the spectrum always has a finite gap; typical examples for negative and positive q are shown in Fig. 2.

3 THE VARIATIONAL APPROXIMATION

Stationary soliton solutions to Eqs. (1) and (2) are sought for in the form $u(z,\tau) = U(\tau)\exp(ikz)$, $v(z,\tau) = V(\tau)\exp(ikz)$ with real U and V, the propagation constant k being an arbitrary real parameter of the soliton-solution family. Substitution of this into Eqs. (1) and (2) leads to the equations

$$(q-k)U + \frac{1}{2}U'' + U^3 + V = 0,\ -(\delta q + k)V - \frac{1}{2}\delta V'' + V^3 + U = 0. \tag{6}$$

Particular exact solutions to Eqs. (6) are available at two special values of the propagation constant, $k = \pm(1-\delta)/\sqrt{-\delta}$, in the form

$$U = \lambda\,\mathrm{sech}\,(\lambda\tau)\,,\ V = \pm\sqrt{-\delta}\lambda\,\mathrm{sech}\,(\lambda\tau)\,, \tag{7}$$

with $\lambda^2 \equiv 2\left(\pm 1/\sqrt{-\delta} - q\right)$. Obviously, these exact solutions exist only at $\delta < 0$, and they are not available in the more interesting range, $\delta > 0$ (with the opposite dispersions in the two cores).

Although exact solutions do not exist at $\delta < 0$, we may find approximate soliton solutions by means of the VA, using the simplest Gaussian *ansatz* (trial wave form),

$$U = A\,\exp\left(-\tau^2/2a^2\right),\ V = B\,\exp\left(-\tau^2/2b^2\right), \tag{8}$$

where A, B and a, b are the amplitudes and widths of the two components of the soliton. The advantage of the Gaussian ansatz is that it will allow the components U and V to have different widths. This feature, as recently demonstrated for the asymmetric DCF [9], can dramatically improve the accuracy of an variational approximation, (VA), over that of the more traditional sech ansatz [8], which is limited to the case of strictly equal widths.

Once the ansatz is adopted, the next step is to substitute it (8) into the Lagrangian density corresponding to Eqs. (6), and then integrate the density over τ, in order to obtain the corresponding *effective Lagrangian.* Then, by varying the free parameters A, B, and a, b

in the latter, one can obtain the variational equations. After some algebra, one can eliminate the amplitudes in favor of the widths, obtaining

$$\begin{aligned} A^2 &= \frac{(3b^2+a^2)+4(k-q)a^2\left(b^2-a^2\right)}{\sqrt{2}a^2\left(3b^2-a^2\right)}, \\ B^2 &= \frac{\delta\left(3a^2+b^2\right)+4(k+\delta q)b^2\left(b^2-a^2\right)}{\sqrt{2}b^2\left(b^2-3a^2\right)}. \end{aligned} \tag{9}$$

The remaining equations determine the widths:

$$\left[3-4(k-q)a^2\right]\left[3\delta+4(k+\delta q)b^2\right]=32(ab)^3\frac{\left(b^2-3a^2\right)\left(3b^2-a^2\right)}{\left(a^2+b^2\right)^3}, \tag{10}$$

$$\frac{\left[3-4(k-q)a^2\right]\left(3a^2-b^2\right)^2}{\left[3\delta+4(k+\delta q)b^2\right]\left(3b^2-a^2\right)^2}=\frac{a^3\left[\delta\left(3a^2+b^2\right)+4(k+\delta q)b^2\left(b^2-a^2\right)\right]}{b^3\left[\left(3b^2+a^2\right)+4(k-q)a^2\left(b^2-a^2\right)\right]}, \tag{11}$$

which we shall solve numerically, finding a and b as functions of the control parameters, δ and q, and the arbitrary propagation constant, k.

In order to present the numerical results in a physically visual form, it will be convenient to define E_u and E_v as the energy content of the respective soliton components,

$$\begin{aligned} E_u &\equiv \left(1/\sqrt{\pi}\right)\int_{-\infty}^{+\infty}|U(\tau)|^2\,dt=A^2a\,, \\ E_v &\equiv \left(1/\sqrt{\pi}\right)\int_{-\infty}^{+\infty}|V(\tau)|^2\,dt=B^2b\,, \end{aligned}$$

where we have made use of the particular form of the ansatz (8) (usually, the energy is defined without the multiplier $1/\sqrt{\pi}$, which we have added here for convenience in the use below). We additionally define $E\equiv E_u+E_v$ as the net energy of the soliton. The results obtained by means of the VA will be displayed in the form of the plots of $k(E)$ and E_v/E vs. E [8, 9]. The latter plot will be interesting as it will show the fraction of the soliton's energy stored in the normal-dispersion core, where, in the absence of the coupling to the anomalous-dispersion one, no bright soliton could exist. As for the plot $k(E)$, it will help us to understand general properties of the solitons, and it will also contain some information about the *stability* of the solitons: according to the Vakhitov-Kolokolov (VK) criterion [13], a necessary stability condition is

$$dk/dE>0\,. \tag{12}$$

In Fig. 3, we show results for a typical case when dispersion is anomalous in both cores, $\delta=-0.5$, $q=0$. In this example, the phase-velocity mismatch, q, has been set equal to zero so that we can see, in a pure form, the effects of the dispersion difference between the two cores. For these values of the parameters, the gap corresponds to $k>1$; when $k^2<1$, we have *delocalized solitons* sitting on top of small-amplitude CW's (see details below), and when $k<-1$, the solution is pure radiative and no localization is possible. We recall that

in Ref. [9], where the asymmetry in the DCF model was solely produced by the phase–velocity mismatch, it was described in detail how the bifurcation diagram for solitons of the symmetric DCF [14, 15] changes due to the phase-velocity mismatch. Comparing the present results with those from Ref. [9], we conclude that the difference in the dispersion coefficients produces qualitatively the same effect as the phase-velocity mismatch does. One can also draw conclusions about the stability of the different branches in Fig. 3, combining the VK criterion [13] and the general principle that a tangent bifurcation, that generates two solution branches "from nothing", gives rise to one stable and one unstable branch. Reviewing a number of cases (not shown here) with various negative values of δ, and with both zero and nonzero q, we have concluded that, as long as the dispersions in both cores have the same sign, the bifurcation diagrams for this version of the asymmetric DCF may be regarded as smooth deformations of those for the symmetric model.

In particular, the parts of the branches $k(E)$ in Fig. 3a, that correspond to the true solitons, are where $k > 1$. When $k^2 < 1$, we do not have true (fully localized) solitons, but rather delocalized ones, i.e., localized pulses sitting on a small-amplitude CW. From the viewpoint of the linear analysis developed in the previous section, these delocalized solitons exist at those values of the propagation constant k at which one pair of the frequencies ω given by Eq. (4) is purely imaginary (corresponding to the soliton), while the other pair is purely real (corresponding to the dispersive radiation). Even though the underlying ansatz (8) assumed the pulses to be fully localized, the results produced by the corresponding VA can successfully predict not only the true solitons, but also some of the delocalized ones. As was shown in [9], in the case when the delocalized solitons exist, the VA, originally devised for the search of the true solitons, singles out such weakly delocalized objects which have a *minimum amplitude* of the underlying CW background.

The next case we shall describe is that with $\delta = 0$, i.e., with exactly zero dispersion in the second core. This is a singular case, essentially different from the general ones $\delta > 0$ and $\delta < 0$ (the reason is that the fourth-order system of equations, (6), becomes of the second order when $\delta = 0$). In Figs. 4 and 5, we display the results obtained for $\delta = 0$ and two different values of the phase-velocity mismatch, $q = 0$ and $q = 1$. In Fig. 4, the gaps are at $k > 1$ and $-1 < k < 0$, while in Fig. 5, they are at $k > \frac{1}{2}(\sqrt{5}+1) \approx 1.62$ and $-\frac{1}{2}(\sqrt{5}-1) \approx -0.62 < k < 0$. In each case, the solution branch crossing $k = 0$ has pieces inside of, and outside of the gaps. A noteworthy peculiarity of the situation with $q = 0$ is the absence of the soliton in the semi-infinite gap (see Fig. 1) at the energies $E \leq 3$. The existence of such an "empty" interval was already noted in the first brief consideration of the DCF model with the different dispersions reported in [8]. However, this property strongly depends on the value of the phase-velocity mismatch q. Fig. 5 demonstrates that there is no empty interval at $q = 1$; one also notes, comparing Figs. 4 and 5, that the change of q gives rise to a qualitative change of the general bifurcation diagram at $\delta = 0$. Still, there are features shared by Figs. 4b and 5b: in both cases, the finite gap, unlike the semi-infinite one, is *completely* filled with the soliton solutions, and for practically all the truly localized solitons, the share of the energy in the zero-dispersion core is less than 1/2.

Now, we proceed to the most interesting case with the positive values of δ, corresponding to the normal dispersion in the second core. In a broad range of values of δ and q, e.g., for $\delta = 1$ and $-1 \leq q < 0.2$ (here, the value 0.2 is very approximate), we observe practically the same picture as shown in Fig. 6, which is for $\delta = 1$ and $q = 0.2$. Here there is only one branch of the solution, which always belongs to the gap, $k^2 < 1$. The initial part of this branch, at $0 < E < 4$, is expected to be stable according to the VK criterion (12). After this, the branch becomes almost horizontal. However, because no apparent bifurcation occurs, we would expect this branch to stay stable even at the higher energies, $E > 4$.

In Fig. 7, we display the results for $\delta = 1$ and $q = 1$. There are two qualitative differences from the previous case. First, a branch analogous to that in Fig. 6 is going, essentially, along the border between the gap, $k^2 < 1$, where the true solitons may exist, and the region where the delocalized solitons are expected, $1 < k^2 < 2$. Second, there is an additional branch at small energies. The additional branch does not belong to the gap and corresponds to delocalized solitons. In the next section, a typical example of such a delocalized soliton, obtained by direct numerical methods, will be displayed.

An unexpected result follows from Figs. 6b and 7b: at all the values of the net energy, the energy share in the normal-dispersion core is larger than 1/2. A typical soliton predicted by the VA has, in this case, a narrow component with a larger amplitude in the anomalous core, and a broad component with a smaller amplitude in the normal core. Thus, we encounter a situation in which a bright soliton can keep a major part of its energy in the normal-dispersion core. One should note, however, that the Gaussian ansatz has an essential drawback: it chops off the usual exponentially decaying (monotonic or oscillating) tails of the soliton. A contribution from the tails may change the energy ratio between the two components of the soliton. It is possible to estimate the contribution of the tails to the ratio of the energies of the solitons' two components, in the case where the tails are decaying with oscillations (i.e., the propagation constant belongs to the subgap (5)): looking for a solution to the linearized equations (6) in the form $U, V = (U_0, V_0) \exp(-\lambda|\tau| + i\chi\tau) + \text{c.c.}$ with real λ and χ, one easily finds $|V_0/U_0|^2 = \delta^{-1}$. Thus, one may naturally expect that, in the case (5), the normal component of the oscillating tail would contain more energy than the anomalous one when $\delta < 1$, and vice versa in the case $\delta > 1$. In accord with this, we will see in the next section that a typical example of the soliton of this type (see Fig. 9 below) has nearly equal total energies in the two components in the border case $\delta = 1$.

Lastly, another noteworthy feature obvious in Figs. 6 and 7 is the fact that a part of the finite gap available for the solitons remains empty, without any soliton solution. Note that in the case $\delta = 0$ considered above, it was possible to have a void in the semi-infinite gap, but the finite one was completely filled. On the other hand, in the recent work [6] treating the gap solitons in nonlinear optical media with a *quadratic* (rather than cubic) nonlinearity, it was also found that a considerable part of the corresponding finite gap remains uninhabited by solitons.

4 DIRECT NUMERICAL RESULTS

In order to check the validity of the VA, we searched for true-soliton and delocalized soliton solutions to Eqs. (6) by direct numerical methods. It is relevant to note that, for $\delta < 0$, we also have the particular exact analytical solutions (7). Comparison with the results of the VA has demonstrated that the corresponding approximate solutions are quite close to these exact ones. However, the principal interest here will be to compare the analytical and numerical results when the dispersion of the second core is either zero or normal, i.e., $\delta \geq 0$.

It was predicted in section 3, on the basis of the VA, that the solitons exist at $\delta = 0$. In section 2, it was concluded, on the basis of the linear analysis, that in this case the solitons would have the usual monotonously decaying tails. These predictions are confirmed by the numerical results, a typical example of which is displayed in Fig. 8. In compliance with the result of the VA, the energy in the anomalous-dispersion core is larger than in the zero-dispersion one, see Figs. 4b and 5b.

A novel type of the soliton predicted by the linear analysis for $\delta > 0$ is a soliton with the oscillating decaying tails. The direct numerical solution, an example of which is shown in Fig. 9, corroborates that such solitons really exist. For this figure, we took $k = -0.8$, $\delta = 1.0$ and $q = 0.2$. The amplitudes of the soliton's components were found to be $U(0) = 0.6060$ and $V(0) = -0.5309$, and the energies are $E_u = 0.3440$ and $E_v = 0.3482$, giving an almost perfect 50% split in the energy distribution. Note that although $V(x)$ has a slightly smaller amplitude, it is also slightly wider than $U(x)$, so that the total energy of the normal component is just slightly *larger* than that of the anomalous one.

An interesting feature of Fig. 6b is that, for large energies, it predicts a larger fraction of the energy to be in the normal core. Searching for such a solution turned out to be a difficult numerical problem. We choose to search for an example of such a solitary-wave solution, with this property, by choosing initial amplitudes and an eigenvalue corresponding to an energy of $E = 4.0$, for which the VA predicts $A = 1.48$, $B = -0.95$, $k = 0.065$, $a = 0.56$, $b = 3.10$, and $E_v/E = 0.69$. We searched in this region, keeping $U(0)$ fixed at 1.500 and numerically varying k and $V(0)$, until the localized solution shown in Fig. 10 had been found. The total energy of this numerical solution was then found to be 2.734, far from the sought for value of 4.00, but still significantly above that in Fig. 9. Along with the numerical solution (solid lines), depicted in Fig. 10 is the variationally predicted soliton (dashed lines) for the same value of the total energy, $E = 2.734$. The numerical solution does have $U(0)$ and $V(0)$, but not the other parameters, close to what is predicted by the VA. In particular, the fraction of the energy found numerically in the normal core was 0.516, just barely over 50%, which should be compared to the analytical variational prediction of $E_v/E = 0.585$, and the numerically exact value of k was 0.049, while the VA predicts $k = -0.103$. Generally for the case shown in Fig. 10, the agreement between the numerical solution and analytical approximation is not as good as in Fig. 9. The reason for the difference seems to be a larger fraction of energy in the oscillating tails, which forces the Gaussian ansatz to "stretch itself out", trying to model this pulse. Whence the variational amplitudes are smaller and the

variational widths are larger than that of the exact soution. However, many other features of the exact solution are nevertheless present in the variational solution. Note in particular, the distinctly different widths of the main peaks in the two components of the pulses.

Finally, the VA has also predicted delocalized solitons, existing on top of a CW background, at such values of the propagation constant k when one pair of the corresponding frequencies ω (see Eq. (4) is real, whilst the other pair is imaginary. A typical numerically found example is displayed in Fig. 11, which corresponds to the upper short branch of the solutions in Fig. 7a. Here, the parameters are $\delta = 1.0$, $q = 1.0$, and $k = 1.52$, and the amplitudes of the two components are $U(0) = 0.5356$ and $V(0) = 0.350$. Although only few examples are shown here, we have obtained direct numerical solutions at weveral other points in the parameter space, and have concluded that the selected examples are fairly generic.

5 CONCLUSION

In this work, we have put forward a new nonlinear optical medium which can support bright gap solitons, viz., an asymmetric dual-core fiber with opposite signs of the dispersion in its two cores. Such a fiber can be easily fabricated. To consider the soliton solutions of the corresponding model based on the linearly coupled NLS equations, we combined the analysis of the dispersion relation for the linearized system, the variational approximation for the full nonlinear one, and direct numerical methods (in order to control the validity of the variational approximation). We have found that in the case when the cores are asymmetric but still have the same sign of the dispersion (anomalous), the general picture of the soliton solutions, including their bifurcations and stability, is qualitatively the same as that studied recently [9] in the model with equal dispersion coefficients in the two cores, the asymmetry being accounted for only by a phase-velocity mismatch between them. In particular, the tails of the solitons in this case are always decaying monotonically. A special case is that when the dispersion in one core is exactly equal to zero; in this case, the system's spectrum simultaneously has a semi-infinite gap and a finite one. Proceeding further to the case when the dispersion in one core is normal (and the system has only a finite gap in its spectrum), we have found three nontrivial features of the gap soliton: (i) its tails may be decaying with oscillations, (ii) the energy in its normal-core component may be equal to or larger than the energy of the anomalous-core one, despite the obvious fact that the normal-dispersion core in isolation cannot support any bright soliton, and, (iii) a part of the finite gap available for the soliton solutions remains empty, having no actual solitons inside it. As concerns the oscillating tails, they are not very important for an isolated soliton; however, they could dramatically affect the character of interactions between solitons, giving rise to two-soliton and multisoliton bound states [11]. Finally, we have also found weakly delocalized solitons sitting on a small-amplitude nonvanishing CW background; however, similar states were recently studied in detail in the simpler asymmetric model [9].

It could be also interesting too to consider dark or mixed dark-bright solitons in the

present model. This is, however, beyond the scope of this work.

References

[1] J.E. Sipe and H.G. Winful, Opt. Lett. **13,** 132 (1988); C.M. de Sterke and J.E. Sipe, Phys. Rev. A **38**, 5149 (1988); **43**, 2467 (1990); Opt. Lett. **18**, 269 (1993); D.S. Psaila and C.M. de Sterke, Opt. Lett. **18**, 1905 (1993); B.A. Malomed and R.S. Tasgal, Phys. Rev. E **49**, 5787 (1994); N.G. Broderick and C.M. de Sterke, Phys. Rev. E **52**, 4458 (1995).

[2] D.N. Christodoulides and R.I. Joseph, Phys. Rev. Lett. **62**, 1746 (1989); A.B. Aceves, and S. Wabnitz, Phys. Lett. A **141**, 37 (1989).

[3] U. Mohideen, R.F. Slusher, V. Mizrahi, T. Ergolan, M. M. Kuwata-Gohokami. P.J. Lemaire, J.E. Sipe, C.M. de Sterke, and N.G.R. Broderick, Opt. Lett. **20**, 1674 (1995).

[4] B.J. Eggleton, R.E. Slusher, C.M. de Sterke, P.A. Krug, and J.E. Sipe, Phys. Rev. Lett. **76**, 1627 (1996).

[5] C. Martin de Sterke, B.J. Eggleton, and P.A. Krug, J. Lightwave Technol. **15**, 1494 (1997).

[6] T. Peschel, U. Peschel, F. Lederer, and B.A. Malomed, Phys. Rev. E **55**, 4630 (1997).

[7] Yu.S. Kivshar, Phys. Rev. E **51**, 1613 (1995); C. Conti, S. Trillo, and G. Assanto, Phys. Rev. Lett. **78**, 3241 (1997); H. He and P.D Drummond, Phys. Rev. Lett. **78**, 4311 (1997).

[8] B.A. Malomed, I.M. Skinner, P.L. Chu, and G.D. Peng, Phys. Rev. E **53**, 4084 (1996).

[9] D.J. Kaup, T.I. Lakoba, and B.A. Malomed, J. Opt. Soc. Am. B **14**, 1199 (1997).

[10] G.P. Agrawal. *Nonlinear Fiber Optics* (Academic Press: Boston, 1989).

[11] B.A. Malomed, Phys. Rev. E **51**, R864 (1995).

[12] A. Hasegawa and Y. Kodama, Solitons in Optical Communications (Oxford Univeristy Press: Oxford, UK, 1995).

[13] M.G. Vakhitov and A.A. Kolokolov, Radiophys. Quantum Electr. **16**, 783 (1973).

[14] P.L. Chu, B.A. Malomed, and G.D. Peng, J. Opt. Soc. Am. B **10**, 1379 (1993).

[15] N.N. Akhmediev and A.A. Ankiewicz, Phys. Rev. Lett. **70**, 2395 (1993); N.N. Akhmediev and J.M. Soto-Crespo, Phys. Rev. E **49**, 5742 (1994).

FIGURE CAPTIONS

Fig. 1. The dispersion curves (3) at $\delta = 0$. For the definiteness, the case $q = 0$ is shown.

Fig. 2. The typical dispersion curves (3) at $\delta > 0$ (in this figure, $\delta = +1$): (a) $q = -1$; (b) $q = +1$.

Fig. 3. The soliton's propagation constant k vs. the net energy E (a), and the share of the energy in the second core, E_v/E, vs. E (b), for $\delta = -0.5$ and $q = 0$. In this and following figures, the dashed horizontal lines demarcate the borders between the gaps and the radiation bands as per Eqs. (3) and (4). The parts of the branches $k(E)$ belong to the radiation spectrum correspond to the "delocalized solitons" sitting on a finite-amplitude CW background.

Fig. 4. The same as in Fig. 3 for $\delta = 0$ and $q = 0$.

Fig. 5. The same as in Fig. 3 for $\delta = 0$ and $q = 1$.

Fig. 6. The same as in Fig. 3 for $\delta = 1$ and $q = 0.2$.

Fig. 7. The same as in Fig. 3 for $\delta = 1$ and $q = 1$.

Fig. 8. A numerically found (solid lines) soliton solution to Eqs. (6) with monotonically decaying tails in the case when the second core has no dispersion ($\delta = 0$), along with its variationally predicted counterpart (dashed lines), at $q = 0.3$ and $E = 0.6821$ (these values are the same for the numerical and analytical solutions). The numerical solution has $k = 1.2755$ and $E_v/E = 0.4373$. The corresponding values for the variational solution are 1.2663 and 0.4338.

Fig. 9. A numerically found (solid lines) soliton solution to Eqs. (6) with oscillating decaying tails in the case when the dispersion in the second core is *normal* ($\delta = +1$), along with its variational counterpart (dashed lines) at $q = 0.2$ and $E = 0.3793$ (these values are the same for the numerical and analytical solutions). The numerically found solution has $k = -0.8000$ and $E_v/E = 0.5020$. The corresponding values for the variational solution are -0.8103 and 0.5257.

Fig. 10. A numerically found (solid lines) soliton solution to Eqs. (6) with oscillating decaying tails, in the case when the dispersion in the second core is *normal* ($\delta = +1$), along with its variational counterpart (dashed lines), at higher energies than in the case shown in Fig. 9. The values of the parameters common for the numerical and analytical solutions are $q = 0.2$ and $E = 2.734$. The numerically found solution has $k = 0.04945$ and $E_v/E = 0.5157$. The corresponding values for the variational solution are -0.1031 and 0.5850.

Fig. 11. A numerically found "delocalized-soliton" solution to Eqs. (6) with a nonvanishing CW background at $\delta = 1.0$, $q = 1.0$. For this solution, $k = 1.52$, $U(0) = 0.5356$, and $V(0) = 0.350$.

FIG. 1

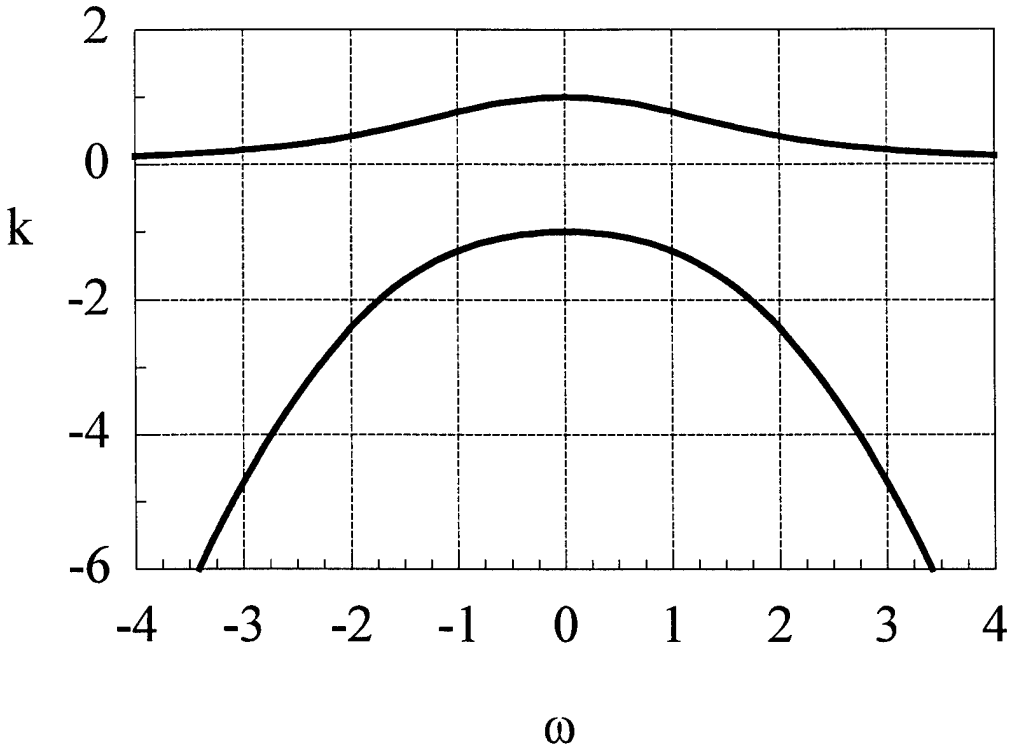

Fig. 2a

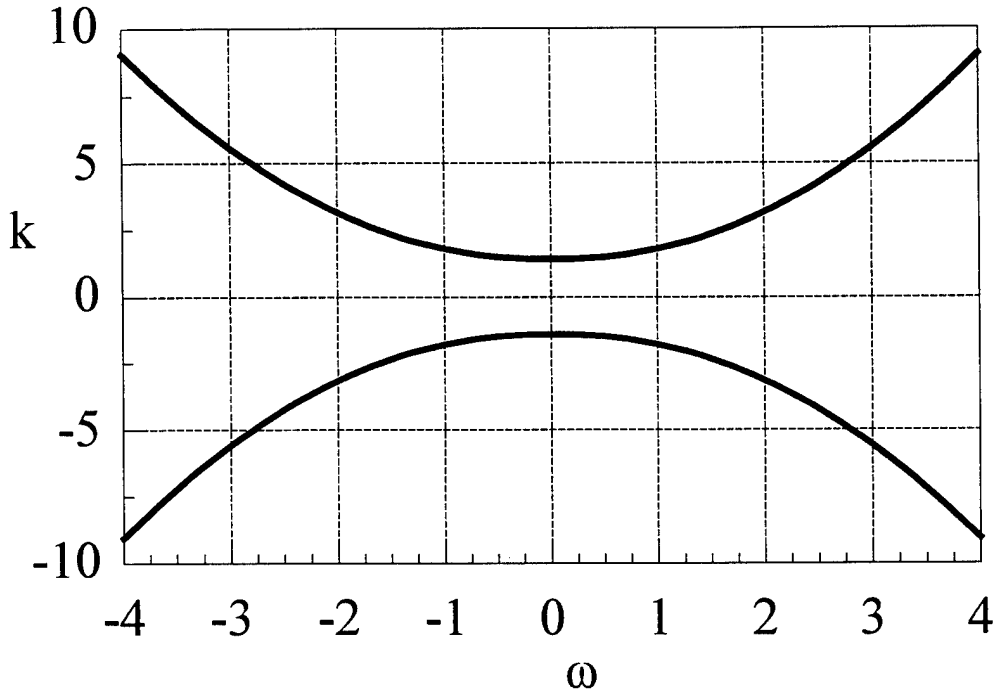

Fig. 2b

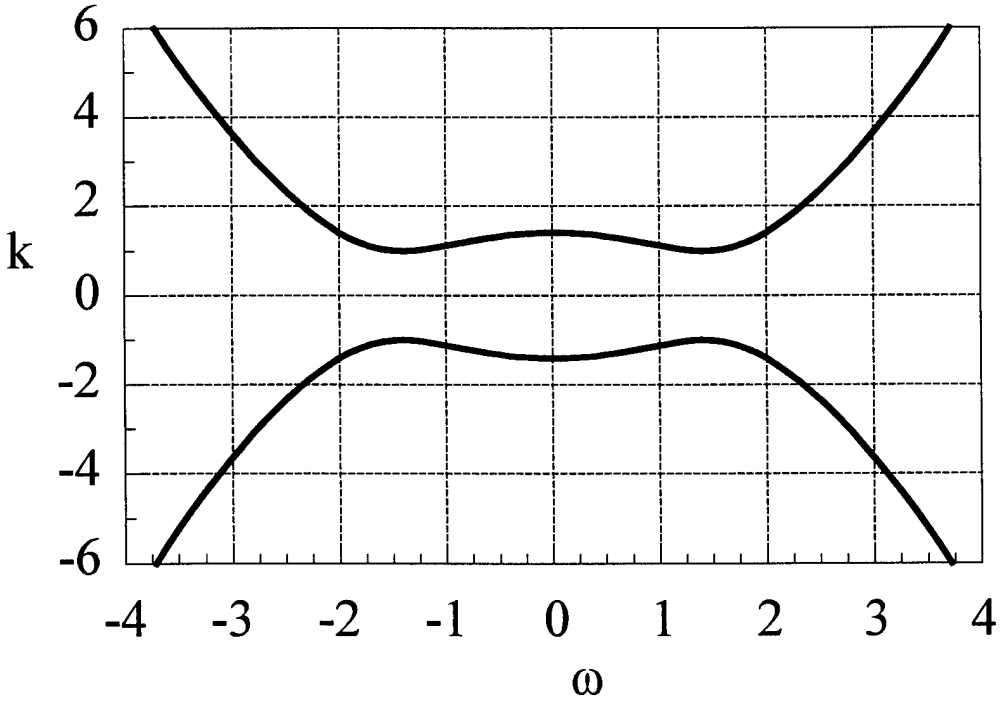

Fig. 3a

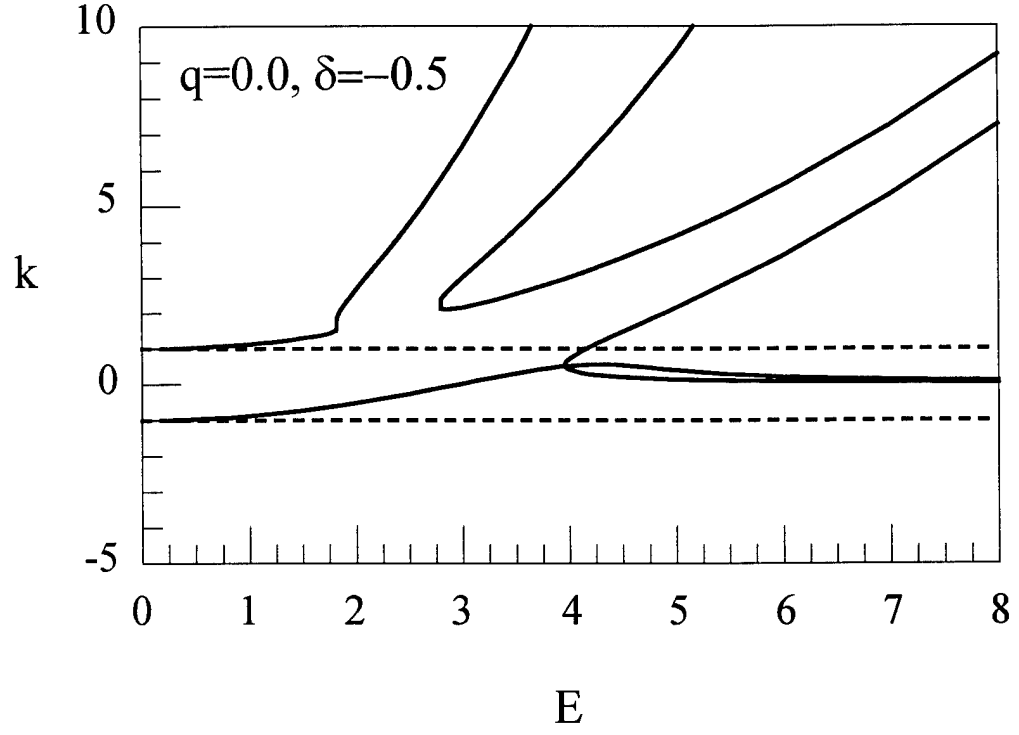
10
5
0
-5
k
q=0.0, δ=–0.5
0
1
2
3
4
5
6
7
8
E

Fig. 3b

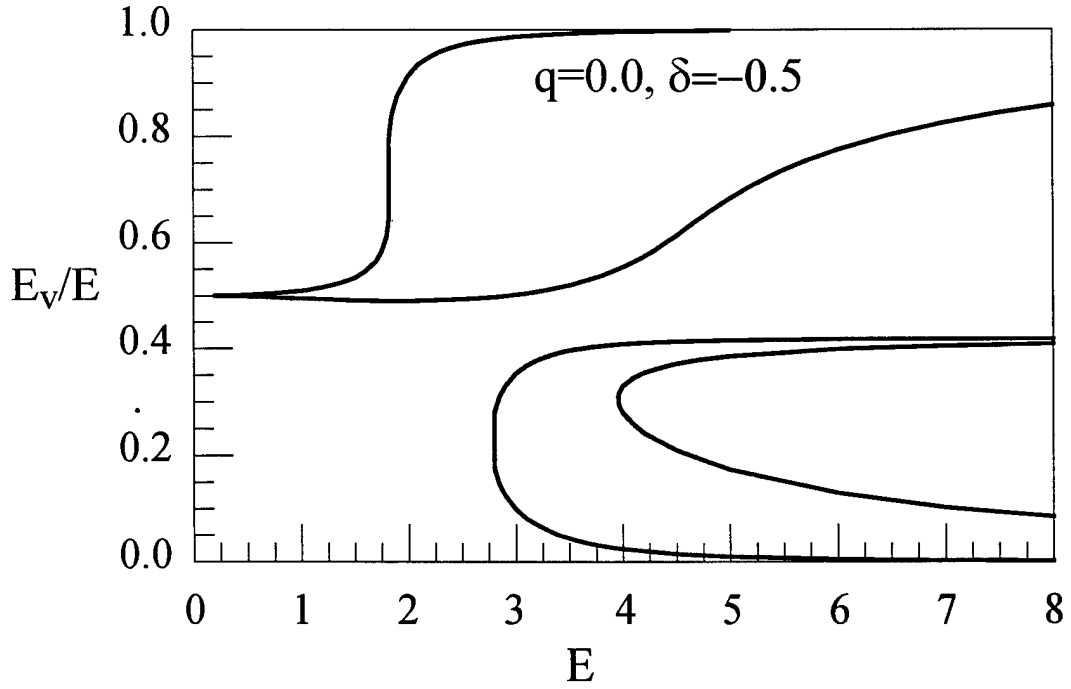
1.0
0.8
0.6
0.4
0.2
0.0
E_v/E
q=0.0, δ=–0.5
0
1
2
3
4
5
6
7
8
E

Fig. 4a

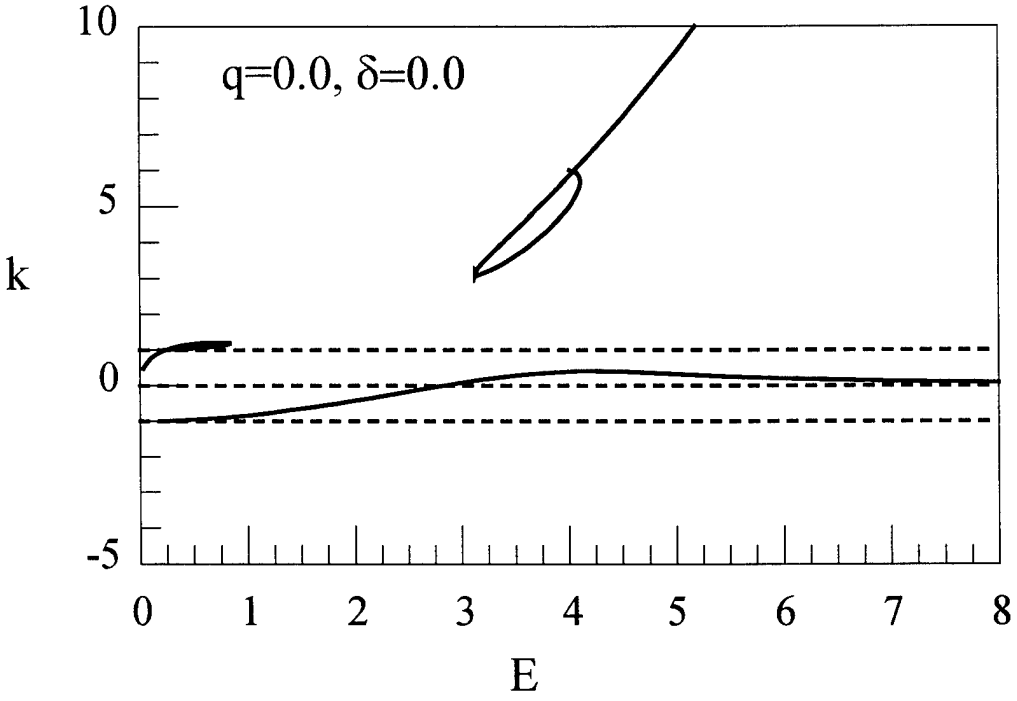
10
5
0
-5
k
q=0.0, δ=0.0
0
1
2
3
4
5
6
7
8
E

Fig. 4b

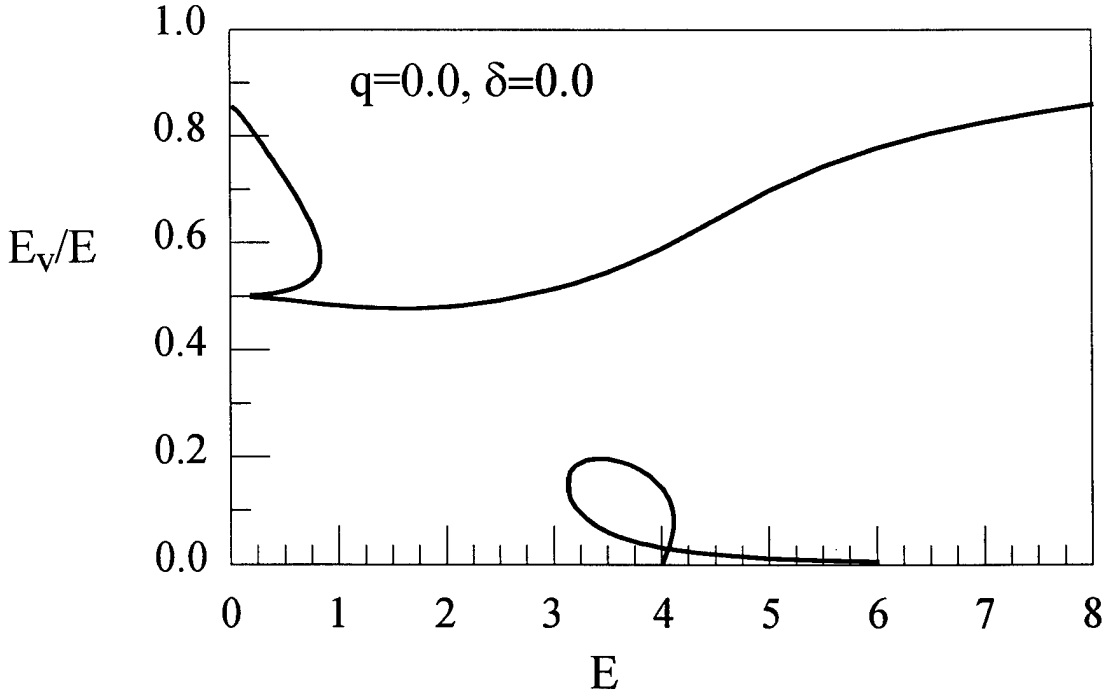
1.0
0.8
0.6
0.4
0.2
0.0
E_v/E
q=0.0, δ=0.0
0
1
2
3
4
5
6
7
8
E

Fig. 5a

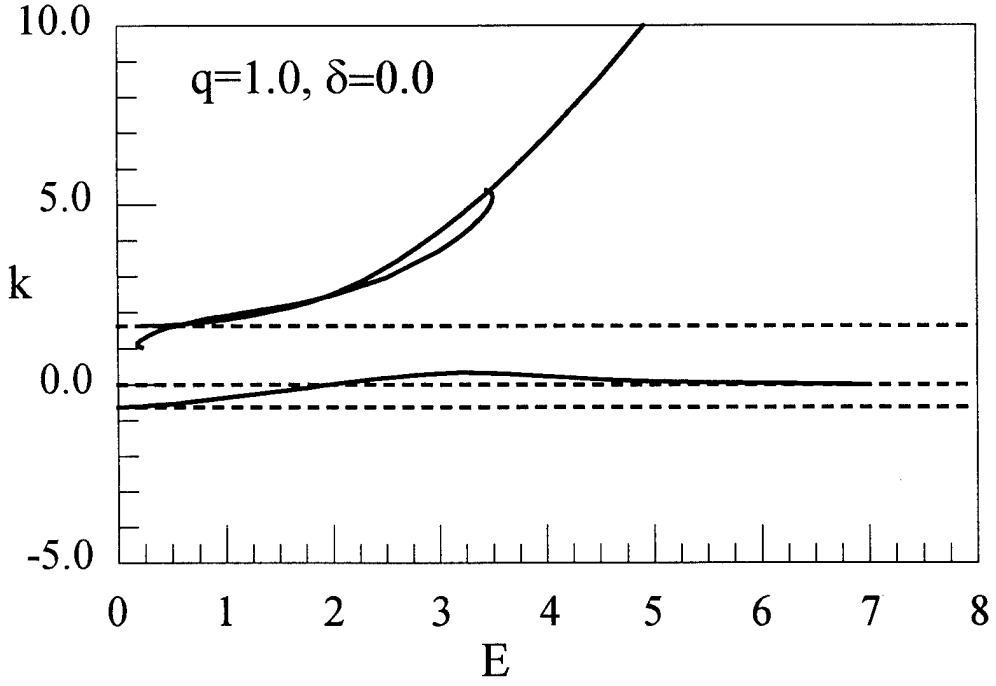
10.0
5.0
0.0
-5.0
k
q=1.0, δ=0.0
0
1
2
3
4
5
6
7
8
E

Fig. 5b

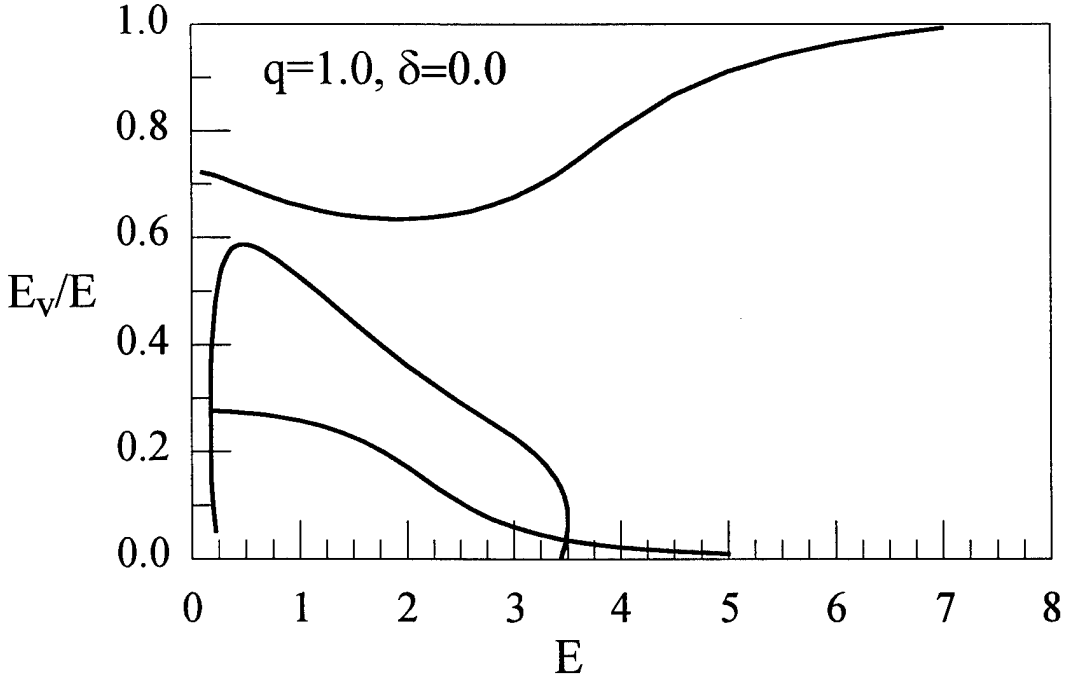
1.0
0.8
0.6
0.4
0.2
0.0
E_v/E
q=1.0, δ=0.0
0
1
2
3
4
5
6
7
8
E

Fig. 6a

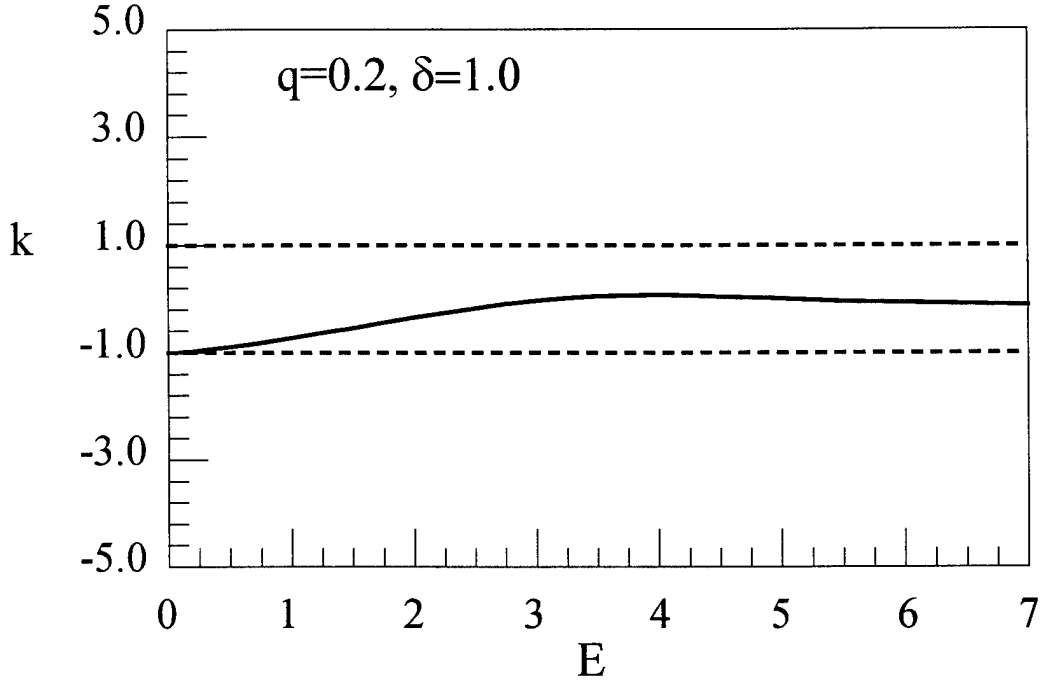
q=0.2, δ=1.0
5.0
3.0
1.0
-1.0
-3.0
-5.0
k
0
1
2
3
4
5
6
7
E

Fig. 6b

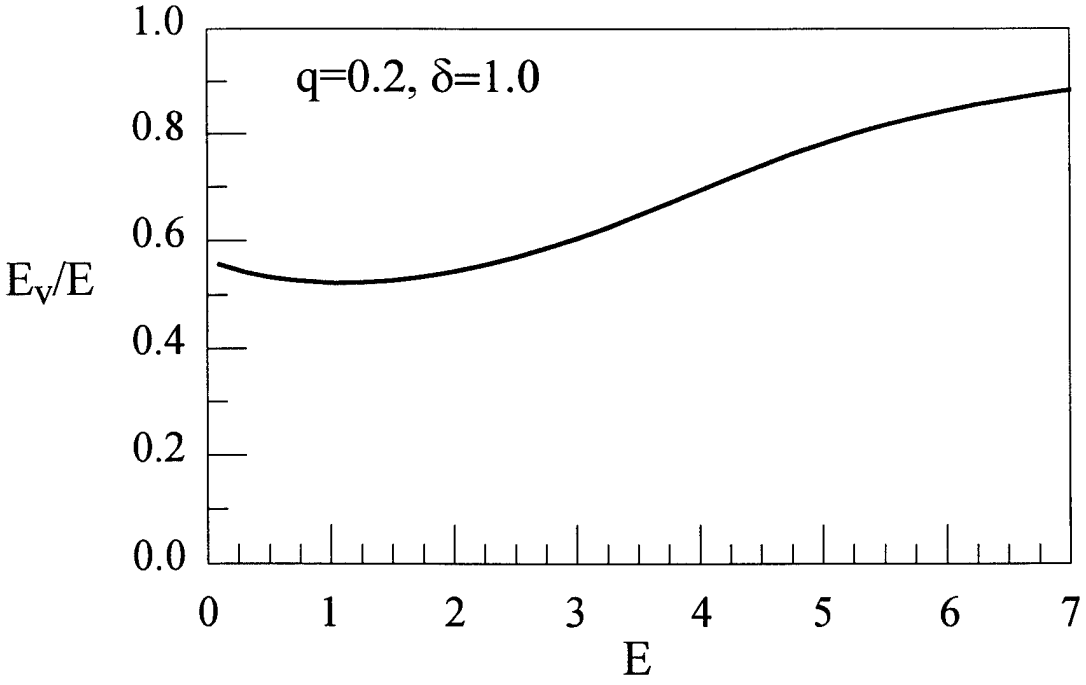
q=0.2, δ=1.0
1.0
0.8
0.6
0.4
0.2
0.0
E_v/E
0
1
2
3
4
5
6
7
E

Fig. 7a

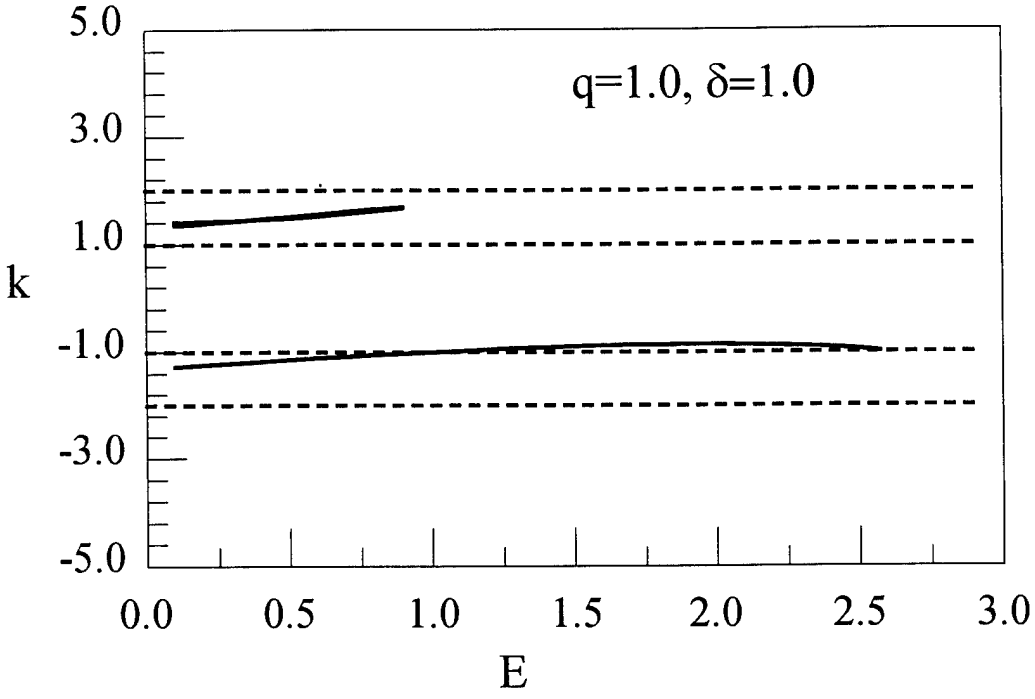
5.0
3.0
1.0
-1.0
-3.0
-5.0
k
q=1.0, δ=1.0
0.0
0.5
1.0
1.5
2.0
2.5
3.0
E

Fig. 7b

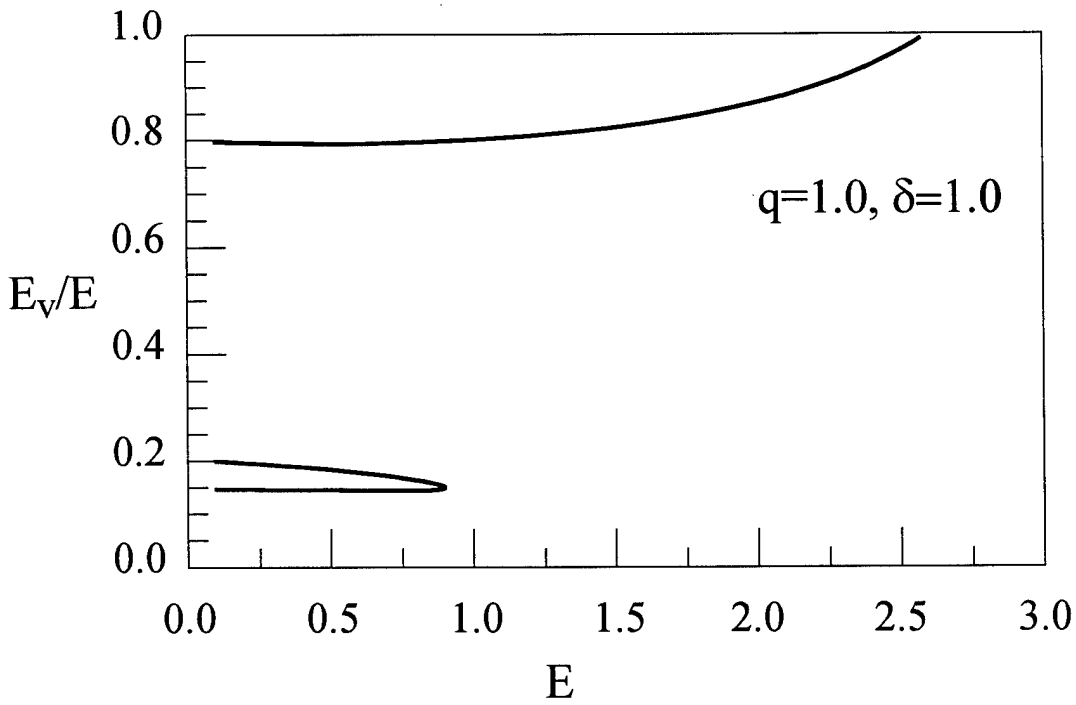
1.0
0.8
0.6
0.4
0.2
0.0
E_V/E
q=1.0, δ=1.0
0.0
0.5
1.0
1.5
2.0
2.5
3.0
E

Fig. 8

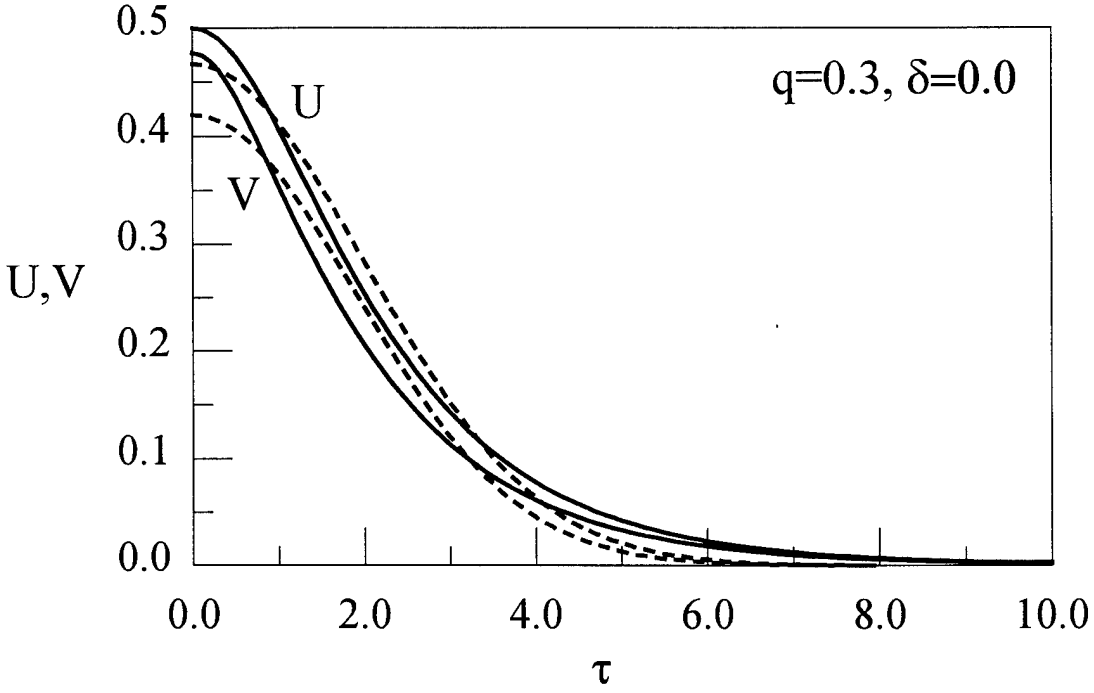

Fig. 9

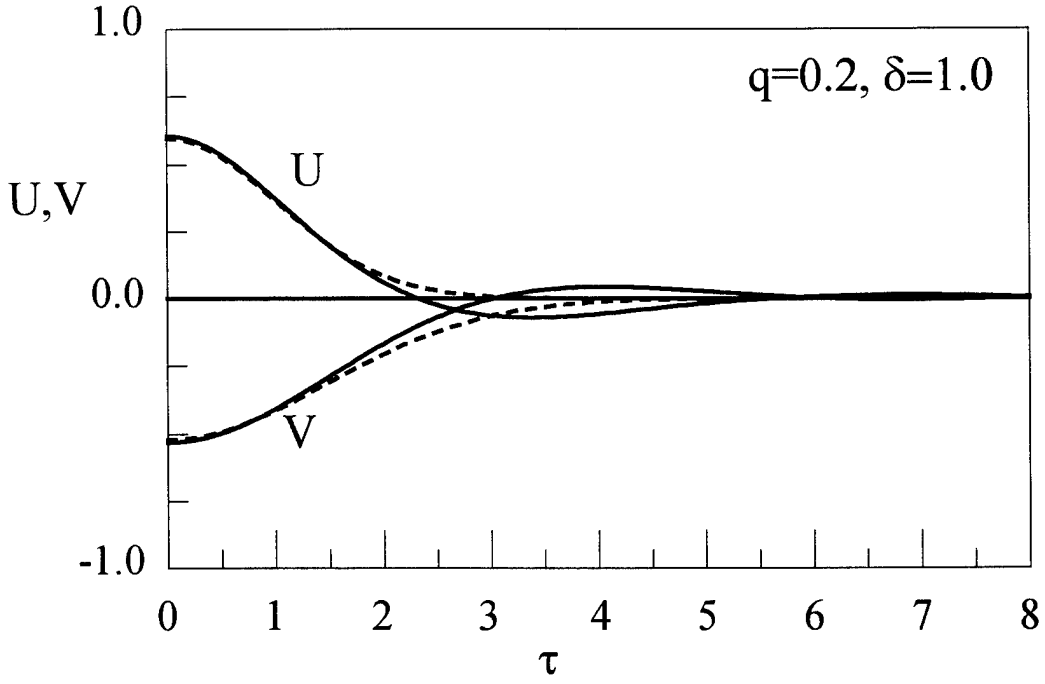

Fig. 10

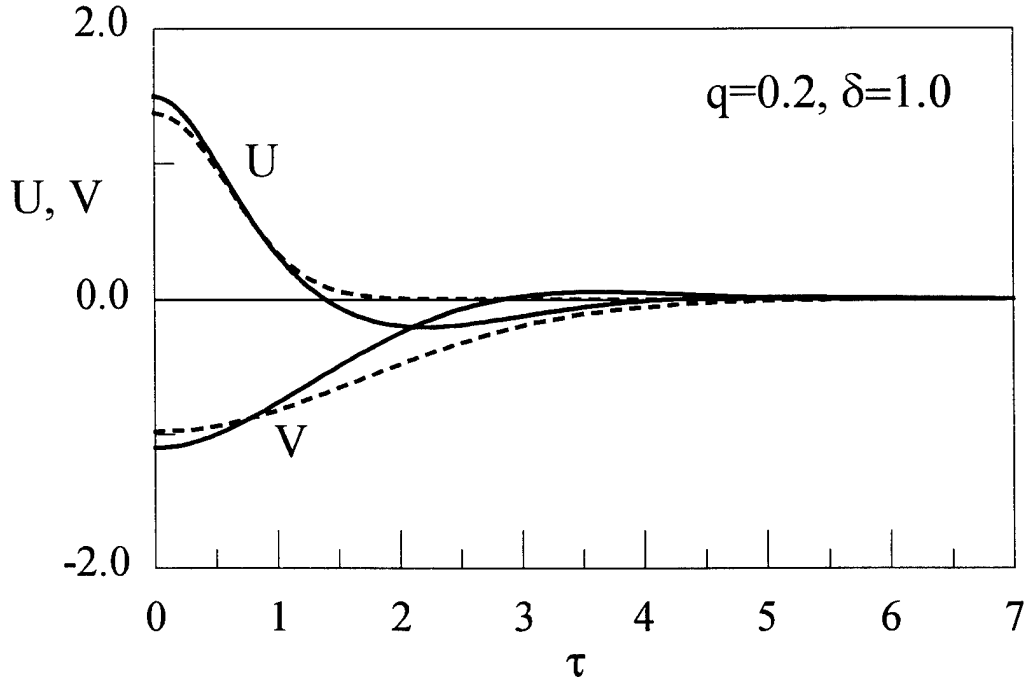

Fig. 11